

Optimizing the lever propelling system for manual wheelchairs

W. CHOROMAŃSKI*, K. FIOK, and G. DOBRZYŃSKI

Faculty of Transport, Warsaw University of Technology, 75 Koszykowa St., 00-662 Warszawa

Abstract. The article concerns the optimization of manual wheelchairs with a lever propelling system. Lever-driven manual wheelchairs are a promising wheelchair group, however they still need to be improved in order to compete successfully with classic manual push rim-driven wheelchairs. Also, despite all manual wheelchairs human work efficiency during propulsion plays an important role, there is not enough research carried out that would focus on this problem regarding lever-driven wheelchairs. The research, presented in this paper, according to the authors' intention, is to make this knowledge gap smaller. The article describes an analytical optimization method for adjusting important lever-drive system parameters – levers length and its axis of rotation position – to individual human anthropometry. The method is based on experimental data regarding maximum human push capabilities acquired in another study. The optimized parameters' values were determined after assessment of maximum human expendable energy during a single work phase (pushing the levers). As a result of this study authors determined optimal levers length and their axis of rotation position for a 50 percentile French male. The carried out research shows also, that the suboptimal area for positioning the levers axis of rotation is relatively wide.

Key words: wheelchair, levers, lever-drive, optimization, propulsion, pushing.

1. Introduction

From all kinds of manual wheelchairs the most popular used today are push-rim driven manual wheelchairs [1]. The nature of the propelling system used in these wheelchairs is already well examined from various points of interest – propelling arm move pattern [2], limb joint dynamics [3], biomechanics and physiology of the propulsion process [4]. Yet there is another wheelchair group that some scientists believe, if sufficiently developed, may significantly improve the quality of motion and thus quality of life of handicapped people, [5–6] – these are lever-driven wheelchairs. There are various existing designs and patents of this type of wheelchairs already carried out. We can divide them into 3 groups according to their design: classic wheelchairs with an attached single lever that propels both wheels [7–8], classic wheelchairs with back wheels replaced by wheels with integrated levers [9–11] and finally specially designed wheelchairs with lever-mechanisms fixed to the wheelchair frame [12–16]. Main advantages of all lever wheelchairs are: their mechanical advantage [5], constant contact of palm with the lever that strongly reduces the risk of hand injury during propulsion, allowing humans to exert force in a more ergonomic and mechanical efficient direction in comparison to classic push rim wheelchairs [4].

Existing lever-driven wheelchair designs differ strongly in proposed lever lengths and their axis of rotation placement in correspondence to a human position on the wheelchair. These differences affect strongly wheelchairs mechanical efficiency as well as their ability to allow humans to exert force in an ergonomic direction. Similar and already examined issue, occurs for classic wheelchairs – parameters like seat height differ between designs and affect strongly human performance during propulsion [17]. Therefore describing these differences with

parameters and optimizing their values can strongly improve existing and future lever-driven wheelchairs independently of their specific designs. The aim of this paper is to present a method for optimizing lever length and its axis of rotation position in correspondence to a human shoulder joint position taking account of individual biomechanical characteristics of human anthropometry. This goal is carried out with the use of an analytical optimization method which is based on experimental data.

2. Methods

In the discussed wheelchair type the power generated by human upper extremities is transmitted to the wheelchairs mechanical drive through a lever system. As previously mentioned the spatial location of the axis of rotation of the lever and its length is under consideration in this work. The issue of optimizing these parameters values was transformed into a task of constrained optimization. A solution of the task can be found either with an experimental or experimental-analytical method. The experimental method consists of measuring the human fatigue caused by propelling a lever wheelchair with variously defined spatial location of the axis of rotation of the lever and its length. In this method the key elements are:

- Creation of a test stand that allows varying the spatial position of the axis of rotation of the lever and its length and applying loads on the lever (simulating resistance to motion) for the given motion conditions;
- Fatigue assessment.

The aim of this method would be defining parameters values (parameters described in point a) in a way which would guarantee human fatigue minimization.

*e-mail: prof.wch@gmail.com

The second possible is the analytical approach. This approach is a subject of here presented article. Authors formulated an optimization task with following simplifying assumptions:

- the velocity of lever motion is not taken into consideration;
- the development of the fatigue process in time doesn't change the optimal values of analyzed parameters;
- the solutions of here presented optimization are independent of load value on the lever;
- out of the whole human work during human-wheelchair interaction only the part associated with pushing the levers is used for wheelchair propulsion.

The authors based their method of solving the task on a heuristic rule stating that the most ergonomic position of human arm while generating the force, so the one that causes least fatigue, is the one in which the possible human arm generated force is maximum.

As a consequence of accepting the presented rule the optimization criteria was defined as maximum energy that human arm can expend according to the general equation (1):

$$W = \vec{F} \cdot \vec{s} = \int_C \vec{F} \cdot d\vec{s}, \tag{1}$$

where W – energy expended by the human arm during a single work (push) phase; \vec{F} – human arm push force vector (varies with arm position); \vec{s} – hand displacement vector; C – path traversed by the human hand; $d\vec{s}$ – position vector.

It is important to notice that in (1) force F changes with lever motion (change in lever position implies change in human arm position). The relation between force and human arm position can be described by mathematical equations derived from experimental data with use of regression analysis. Since this article benefits from such equations, therefore here presented analytical optimization method is in fact an experimental-analytical method.

Authors assume that in here discussed lever wheelchair the integration trajectory C will always be a part of a circle, that will vary only with change in position of the axis of rotation of the lever and lever length.

Therefore defining maximum human arm push forces as a function of various arm position becomes a vital issue.

2.1. Force component – the human arm push force vector.

In the assumed lever-driven wheelchair concept the wheelchair is propelled by pushing levers by human arms. Performing optimization of wheelchairs design parameters requires knowledge of force, that human can expend while pushing levers. The issue of describing maximum human expendable forces with use of upper extremities is a complex problem. There was a lot of research carried out which aimed to find maximum human expendable forces while conducting different tasks with use of upper extremities, for example performing hand grip [18–22] or using a screwdriver [23]. Most authors

tend to determine these maximum forces during experimental measurement of individuals. Researchers concluded, that these values of forces vary strongly depending on the carried out activity and a human arm position while conducting the given task. Therefore, for a given task, in this case pushing the levers, maximum push forces that human can expend vary strongly with human arm position. In this paper, it was decided to benefit from experimental-analytical research in which the relation between maximum human expendable arm force while pushing and human arm position was described with mathematical formulas applicable for the entire human arm reachable area.

The value of human arm push force in presented optimization method is calculated with use of Eqs. (2) and (3) incorporated from a foreign study [24].

$$F_{mp} = 0.07584 \cdot F_p \cdot (\sin 1, 3 \cdot (q_7 + 65^\circ) + 2.333) \cdot (\sin 3 \cdot (q_5 + 28^\circ) + 4.835) \cdot (\sin 2.3 \cdot (q_1 + 33.5^\circ) + 9.466) \cdot (\sin 2 \cdot (q_2 + 22^\circ) - 4.646) \cdot (\sin(q_3 - 50^\circ) - 4.24849), \tag{2}$$

$$F_p = 1 + 0.18 \cdot \cos(0.5 \cdot q_4) + 0.435 \cdot \sin q_6 - 0.3724 \cdot \cos^2(0, 5 \cdot q_4) - 0.669 \cdot \cos(0.5 \cdot q_4) \cdot \sin q_6 - 1.022 \cdot \sin^2 q_6. \tag{3}$$

In these equations force value is derived directly from human arm position in 3D which is described basing on a simplified human arm model consisting of 3 rigid bodies corresponding to arm, forearm, palm and 3 joints allowing motion that can be described with 7 Degrees of Freedom (DOFs: shoulder joint – 3 DOFs, elbow and wrist joints – 2 DOFs each). In Eqs. (2) and (3) variables from q_1 to q_7 represent these 7 DOFs. The simplified arm model along with possible arm motion in the incorporated model are presented in Fig. 1 and Fig. 2.

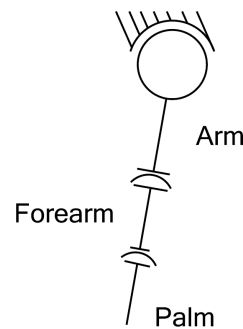


Fig. 1. Simplified 7 DOF human arm model. Assumptions: shoulder joint – 3 DOFs, joints between arm-forearm and forearm-palm – 2 DOFs each

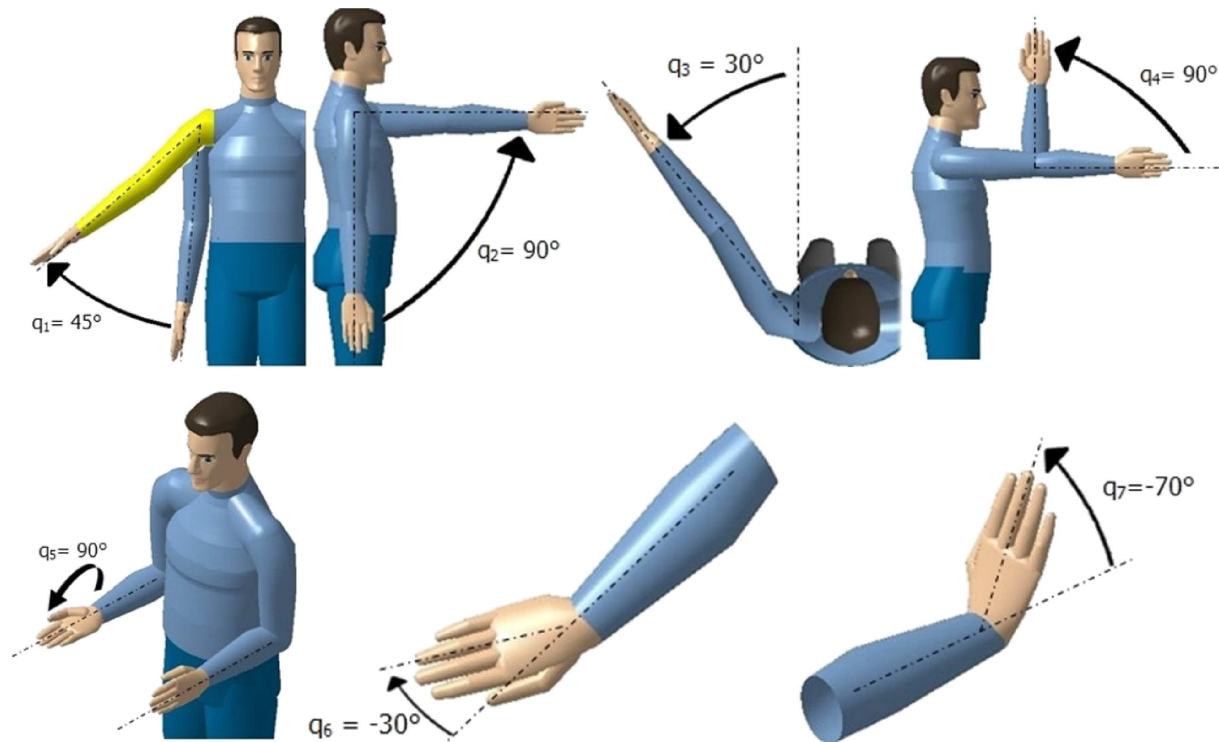


Fig. 2. Definitions and example values of possible arm motion in the analyzed human arm model. Each of DOFs is corresponding to parameters from q_1 to q_7

Equations (2) and (3) were derived from experimental data [24] and describe maximum human arm push force values. In her experiment the push force was assumed to be parallel to the forearm. The experiment which provided necessary data was carried out on 12 young males (aged 26–31, mean 28.8 years) who were 172–185 cm high (mean 176.8 cm) and weighed from 62 to 89 kg (mean 73 kg). Each of the subjects was asked to expend maximum push force in 24 defined positions for 3 seconds. As a result Roman-Liu acquired knowledge about 24 maximum push force values in 3D space. Next step of her study was to find equations based on 7 variables (7 DOFs of the human arm model) that would mathematically connect information about the force values and human arm spatial orientation. The results given by Roman-Liu are the already mentioned Eqs. (2) and (3) based on trigonometric functions. The Spearman’s correlation coefficient between the push force values acquired in her experiment and developed equations was calculated and equals to 0.94. The mean maximum push force for each of the 24 human arm positions from both experimental data and results acquired from Eqs. (2) and (3) are presented in Fig. 3.

It is worth mentioning, that using relatively small sample size (12 persons) for deriving formulas (2) and (3) does not limit the range of applicability of the here presented optimization method. The spread of maximum push forces inside the analyzed sample expressed by the standard deviation was high and achieved levels of 25–30% of mean value. In the given issue, optimizing wheelchair parameters individually requires deriving formulas (2) and (3) for each wheelchair user, which will probably cause slight differences when compared to the

above presented F . In this article the discussed formulas (2) and (3) are derived from averaged data and were used for demonstration of results that can be achieved with use of here presented optimization method.

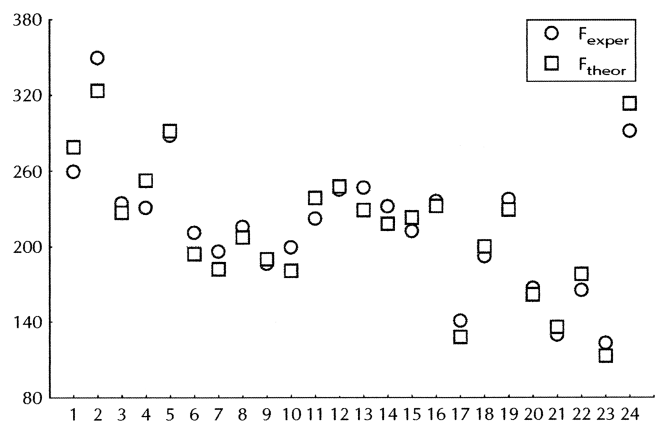


Fig. 3. Comparison of maximum push force values gathered in the experiment (F_{exper} – circles) and estimated from Eqs. (2) and (3) (F_{theor} red rectangles). On the x axis 24 arm positions are listed, on the y axis corresponding maximum push force values are visible [24].

2.2. Adapting 3D arm model to a 2D levers’ work plane.

Since in a lever-driven manual wheelchair levers move only forwards and backwards on the sagittal plane, the authors decided to perform an analysis in 2D instead of 3D. Thus in the above presented human arm model certain assumptions regarding its parameters’ values were made. Firstly, that $q_1 = q_3 = q_5 = 0^\circ$ which assured that arm movement takes

place on the desired plane (different combinations of these values allow defining all planes in 3D space). Secondly, that $q_6 = q_7 = 0^\circ$, which assured that no wrist movement is allowed (this assumption makes lever propulsion system more healthy and accessible to a wider handicapped people group). Thirdly, q_2 and q_4 were left variable – these parameters guarantee that all points located in human arms’ range on the desired plane are reachable. Presented assumptions limited somewhat this methods application but at the same time allowed creation of a schema of the analyzed work plane which is presented in Fig. 4.

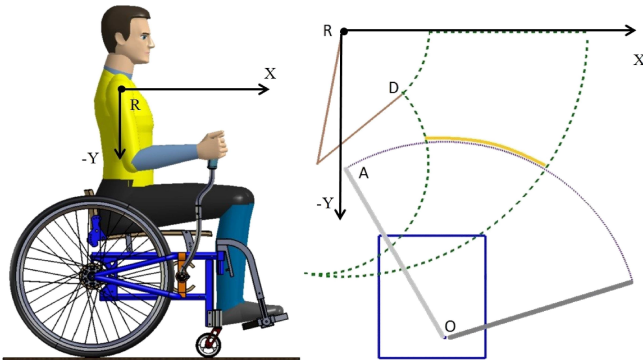


Fig. 4. Schema of the analyzed work plane and a lever-driven wheelchair model. Legend: **R** – shoulder joint position and origin of the XY coordinate system; **O** – levers axis of rotation position; **A** – levers end; **|OA|** - levers length; **D** – exemplary palm position; **brown lines** – exemplary arm and forearm position; **area enclosed by green broken lines** – human arm reachable area; **grey lines** – 2 extreme lever positions; **violet arc** – arc spanned by the levers end; **yellow line** – hand movement pattern when pushing the lever; **blue rectangle** – analyzed area for placement of levers axis of rotation

2.3. Maximum push force values on the analyzed work plane. Maximum push force values were calculated taking into account values of q_2 and q_4 derived from human arm movement capabilities and rational boundaries. The assumed values were q_2 in range $(-10^\circ; 90^{circ})$ and q_4 in range $(0^\circ; 140^\circ)$. One boundary of the q_2 variable was chosen as -10° according to authors observation of manual wheelchair users during their regular movement – it seems that handicapped people rarely achieve values lower than -10° . The other boundary, (90^{circ}) was chosen in order to inhibit repeatable expending of push force with the palm located over the shoulder joint as it causes very high physical strain. Limitations of q_4 variable were determined by the anatomical limitations of human forearm movement [25]. Moreover in this paper all calculations were performed for a 50 percentile French male, hence arm and forearm lengths taken into consideration where respectively 32.84 cm and 27.14 cm. The result of the calculations is presented in Fig. 5. White color on the graph indicates, that the desired position was out of reach of the human arm model. Edges of the reachable area are not smooth due to discretization of the analyzed work plane.

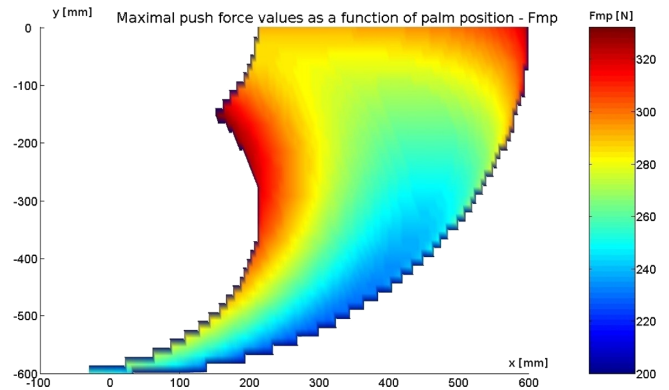


Fig. 5. Maximum push force values on the analyzed work plane (calculated in the area enclosed by green broken lines in Fig. 4). **Point (0;0)** – shoulder joint position; **x [mm]** – horizontal distance between shoulder joint and palm (values less than 0 indicate that the palm is situated behind the shoulder joint); **y [mm]** – vertical distance between shoulder joint and palm (values less than 0 indicate that the palm is situated under the shoulder joint); **F_{mp} [N]** – maximum expendable push force value as a function of palm position

2.4. Human-expendable energy calculation. As previously mentioned, the optimization method in this paper is based on knowledge of the human-expendable energy in a single push phase. The quantity of this energy was first given by equation (1). With the assumptions presented above this equation was developed into equation (4) which allowed calculating the desired energy values for optimization of the wheelchairs lever propulsion system.

$$W_{x_{oi}y_{oj}}^{l_h} = \int_{a_1(l_h, \beta)}^{a_n(l_h, \beta)} F_{mp}(q_2, q_4) \cdot \cos(q_2 + q_4 - 90^\circ) \cdot l_h \cdot \sin \beta d\beta \quad (4)$$

$W_{x_{oi}y_{oj}}^{l_h}$ – maximum energy transfer in a single stroke with previously defined levers axis of rotation position $O(x_o, y_o)$ and levers length (l_h); $O = \{o1, o2, \dots, ok\}$ – set of analyzed levers’ axis of rotation positions, there were 224 positions analyzed (combinations of x_o and y_o , in Fig. 4 blue rectangle limits the analyzed positions of O); $X_o = \{xo1, xo2, \dots, xoi\} = \{90, 110, 130, 150, 170, 190, 210, 230, 250, 270, 290, 310, 330, 350\}$ – set of coordinates describing levers’ axis of rotation position horizontally [mm] in correspondence to shoulder joint position, according to authors knowledge this range of values can represent the range of possible horizontal axis placement in existing lever-driven wheelchairs. Since in some designs lever and back wheel axes of rotation are coincident and wheelchair users usually have their shoulder joint positioned slightly behind the axis, thus authors assumed that levers’ axis of rotation in this study will not be closer than 90 mm to the shoulder joint. The second limit of 350 mm was derived from the fact that often the wheelchairs frame shape inhibits designers will to place the axis of rotation more to the front; $Y_o = \{yo1, yo2, \dots, yoj\} = \{-500, -520, -540, -560, -580, -600, -620, -640, -660, -680, -700, -720, -740, -760, -780, -800\}$ – set of coordinates describing levers’ axis of rotation position vertically [mm] in correspon-

dence to shoulder joint position, according to authors knowledge this range of values can represent the range of possible vertical axis placement in existing lever-driven wheelchairs; β – angle describing levers position, analyzed angles where in range of 103° , in Fig. 4 the violet arc spanned between 2 grey lines – boundary lever positions – has to go through the whole area limited by green dotted line – the range of palm motion. To meet this condition, for every analyzed point O , the angle range should be 103° . It is important to understand that this does not mean that in each push phase the lever is rotated for 103° ; $L = \{l_1, l_2, \dots, l_n\} = \{390, 420, 450, 480, 510, 540, 570, 600, 630, 660\}$ – set of 10 analyzed levers' lengths [mm], this range of values was chosen according to authors knowledge of existing lever-driven wheelchairs; $A = \{a_1, a_2, \dots, a_n\}$ – set of points corresponding to palms positions when pushing the lever (function of levers' length L and levers' position described by O and β , during each push phase there were 51 palms positions considered, in Fig. 4 point A is the first of 51 considered palms positions). The amount of 51 palms positions considered comes from the discretization assumed during mathematical calculations.

The above equation describes the phenomena of human arm pushing a lever with palm moving from point a_1 to a_n , where a_1 is the first and a_n is the last reachable point. Applying maximum possible push force F_{mp} over arc spanned between these points generates measurable energy transfer.

As previously stated, some of the geometric parameters in the energy calculation process were limited according to authors knowledge of lever-driven wheelchairs. This limitation can hinder the instant use of presented results for some specific lever-driven wheelchairs. However, this should not be a major problem since it is possible to change the range of analyzed variables if necessary. By analogy, the method allows changing previously assumed limits of human arm motion (parameters q_2 and q_4) to adjust them to a specific biomechanical limitations of a disabled individual.

3. Results

Results of the performed calculations are presented in Figs. 6, 7 and 8. Figure 6 is divided into 10 sub-graphs where all calculated energy values are presented: each of the sub-graphs is showing various maximum human-expendable energy as a function of lever axis of rotation position for a fixed lever length (10 sub-graphs are corresponding to 10 analyzed lever lengths).

Figure 7 was created according to a following algorithm: firstly, choose 1 lever axis of rotation position, secondly, compare 10 values (derived from 10 lever lengths) of energy associated with this position, thirdly, choose the highest of this values, show it on the graph and repeat from the beginning for another lever axis of rotation position.

According to the assumed optimization criteria an optimal combination of parameters is the one that guarantees the highest of all maximum human-expendable energy (highest

value in Fig. 7). This requirement is met by a combination of parameters: lever axis of rotation moved 350 mm in front ($x = 350$) of and 740 mm under ($y = -740$) the shoulder joint along with the levers' length 600 mm ($l = 600$).

4. Discussion

Here presented optimization process provides information not only about a single optimal combination of analyzed parameters, but also about the possible suboptimal combinations. As presented in Fig. 6, for every lever length there is a certain suboptimal area for levers axis of rotation placement. If we agree that it is the red and dark-red-colored area (sub-maximum energy values), then it is possible to say that there are many 'good' positions of lever axis of rotation for every lever length. This knowledge can be useful in a lever-driven wheelchair construction process.

On the other hand, Fig. 7 shows that regardless lever length, the further from the shoulder joint is the levers axis of rotation positioned, the better. The highest calculated energy values occur when $x = 350$ or close to it, which could incite to perform further calculations with higher x values. However, as already mentioned, authors find the confines of this study reflecting the present day needs of lever-driven wheelchair designs. If a designer finds it reasonable, it is always possible to enhance this methods limits.

Figure 8 was created in order to present the differences between maximum and minimum energy values for 10 fixed lever lengths. This comparison shows that a lot of improvement can be made in positioning lever axis of rotation for every lever length, f. e. if we analyze the shortest lever – 390 mm – we can show that the difference between maximum and minimum energy values is way over 100%. At the same time we can observe that the differences between maximum energy values for all lever lengths are very small, not higher than 10%. This fact brings us to a conclusion that lever length is not a key factor in lever wheelchair design optimization if we manage to position the levers axis of rotation properly.

However, before applying results shown in this analyze one must always remember, that it was prepared for a 50 percentile French male, which means that there were certain arm and forearm lengths assumed. It is obvious that for different anthropometric parameters, this analyze will be false. Luckily, here presented method allows adapting to such differences. When one is willing to use this method f.e. for 10 percentile Dutch male, all he must do is adjust the methods parameters to the specific human anthropometry. In the method it is also possible to change the limits of human arm movement (parameters q_2 and q_4) proposed by the authors, which can help adjusting the calculations to specific abilities of wheelchair users. Wheelchair designers willing to limit or enhance the possible lever rotation angle can also profit from adjusting parameter β according to their desires. Similar changes can be proposed if a certain lever length (parameter L) or lever axis of rotation position (parameters x_0 and y_0) are desired.

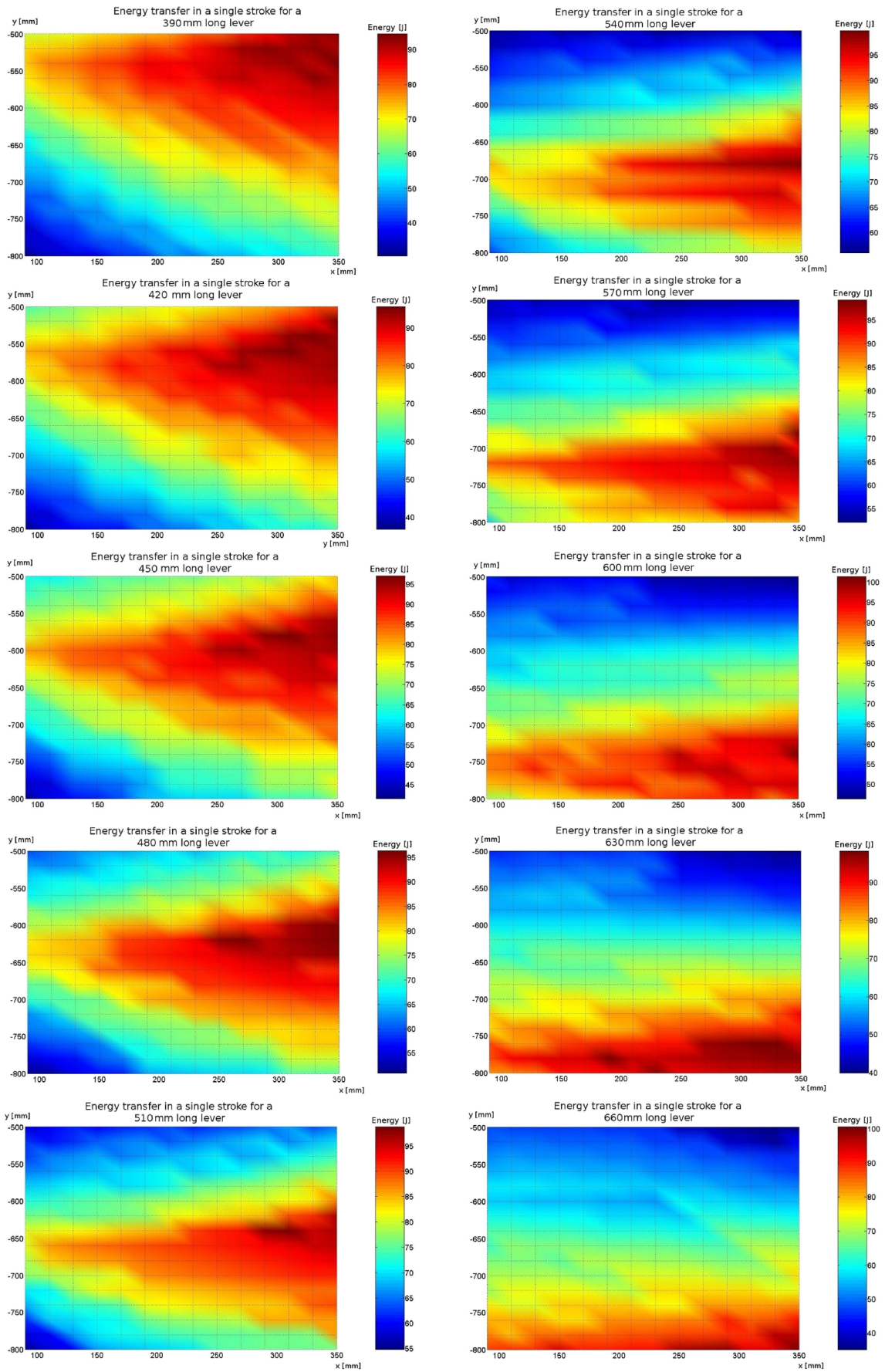


Fig. 6. Maximum energy transfers in a single stroke for 10 lever lengths and various levers axis of rotations position

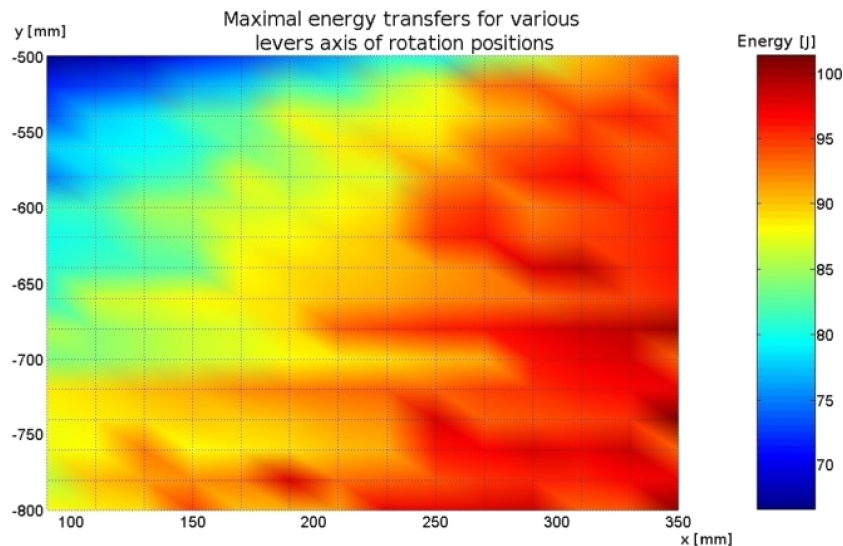


Fig. 7. Maximum energy transfer in a single stroke for various levers axis of rotation positions and different levers lengths (10 lever lengths for each axis of rotation position where considered, from these 10 results for each axis of rotation position the biggest energy transfer is shown; this graph does not indicate what was the levers length which allowed here presented energy transfer)

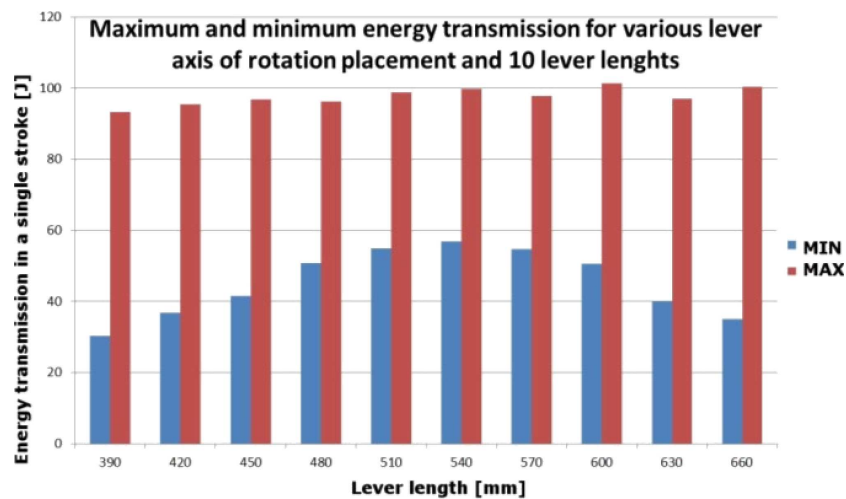


Fig. 8. Comparison between maximum and minimum energy values that human can expend in a single push faze for 10 lever lengths with various position of lever axis of rotation

Results from the optimization method presented in this paper can be a guideline for lever-driven wheelchair designers. However before fully accepting them, an experimental validation of these results should be performed. Authors present day aim is to construct a test stand that will allow verifying here presented findings.

Acknowledgements. This article was financed from the ECO-Mobility project WND-POIG.01.03.01-14-154/09. The project was co-financed from the European Regional Development Fund within the framework of Operational Programme Innovative Economy.

REFERENCES

[1] L.H.V. Van der Woude, A.J. Dallmeijer, J. Annet, T.W.J. Janssen, W.J. Thomas, and H.E.J. Veeger, "Alternative modes

of manual wheelchair ambulation: an overview", *Am. J. Physical Medicine & Rehabilitation* 80, 765–777 (2001).
 [2] L.A. Rozendaal, H.E.J. Veeger, and L.H.V. van der Woude, "The push force pattern in manual wheelchair propulsion as a balance between cost and effect", *J. Biomechanics* 36, 239–247 (2003).
 [3] G. Desroches, R. Dumas, D. Pradon, P. Vaslin, F.X. Lepoutre, and L. Cheze, "Upper limb joint dynamics during manual wheelchair propulsion", *Clinical Biomechanics* 25, 299–306 (2010).
 [4] L.H.V. Van der Woude, H.E.J. Veeger, A.J. Dallmeijer, T.W.J. Janssen, and L.A. Rozendaal, "Biomechanics and physiology in active manual wheelchair propulsion", *Medical Engineering & Physics* 23, 713–733 (2001).
 [5] L.H.V. Van der Woude, E. Botden, I. Vriend, D. Veeger, "Mechanical advantage in wheelchair lever propulsion: effect on physical strain and efficiency", *J. Rehabilitation Research and Development* 34, 286–94 (1997).

- [6] A. Rifai Sarraj, R. Massarelli, F. Rigal, E. Moussa, C. Jacob, A. Fazah, and M. Kabbara, "Evaluation of a wheelchair prototype with non-conventional, manual propulsion", *Annals Physical and Rehabilitation Medicine* 53, 105–117 (2010).
- [7] G. Harris, B. Ralph, and L.R. Bradshaw, U.S. Patent #5020815, *One-Arm Lever Propulsion Accessory* (1991).
- [8] <http://www.invacare.com.au>, *Invacare One Arm Driven by Lever*, Invacare Australia Pty Ltd.
- [9] <http://www.wijit.com>, Wijit, 2270 Douglas Blvd., Suite 212 Roseville, CA 95661.
- [10] <http://www.leverdrive.com>, *Lever Drive, Cortical Sysematics LLC*.
- [11] <http://triomobility.com>, Rio Mobility Company, 2325 3rd St., Ste 242 San Francisco, CA 94107. *Pivot Dual Lever Drive*.
- [12] <http://www.jouleflow-water-features.com>, Jouleflow Unit 5 Enterprise Court Park Farm Ind. Est. Wellingborough Northamptonshire NN8 6UW.
- [13] <http://www.forethoughtdesigns.com>, *EZ-2 Twin Lever, Cable Drive Wheelchair*, Steven Tidcomb Fore-Thought Designs.
- [14] M. Hanna, U.S. Patent #5007655 – *Sprocket-Rack Arrangement* (1991).
- [15] W. O. Lucken, U.S. Patent #4453729 – *Dual Lever/Ratchet Propulsion Mechanism* (1984).
- [16] Carl F. Drake, U.S. Patent #5941547 – *Dual Lever Drive Cable Propulsion Mechanism* (1999).
- [17] L.H.V. Van der Woude, A. Bouw, J. Van Wegen, H. Van As, H.E.J. Veeger, and S. De Groot, "Seat height: effects on sub-maximal hand rim wheelchair performance during spinal cord injury rehabilitation", *J. Rehabil. Med.* 41, 143–149 (2009).
- [18] M.S. Hallbeck, and D.L. McMullin, "Maximal power grasp and three-jaw chuck pinch force as a function of wrist position, age, and glove type", *Int. J. Industrial Ergonomics* 11, 195–206 (1993).
- [19] B.P. Kattel, T.K. Fredericks, J.E. Fernandez, and D.C. Lee, "The effect of upper extremity posture on maximum grip strength", *Int. J. Industrial Ergonomics* 18, 423–429 (1996).
- [20] L. Lamoreaux and M.M. Hoffer, "The effect of wrist deviation on grip and pinch strength", *Clinical Orthopaedics and Related Research* 314, 152–155 (1995).
- [21] R.J. Marley and R.R. Wehrman, "Grip strength as a function of forearm rotation and elbow posture", *36 Proc. Annual Meeting Human Factors and Ergonomics Society* 1, 791–795 (1992).
- [22] S.W. O'Driscoll, E. Horii, R. Ness, T.D. Cahalan, R.R. Richards, and K.N. An, "The relationship between wrist position, grasp size, and grip strength", *J. Hand Surgery* 17A, 169–177 (1992).
- [23] D.J. Habes, and K.A. Grant, "An electromyographic study of maximum torques and upper extremity muscle activity in simulated screwdriving task", *Int. J. Industrial Ergonomics* 20, 339–346 (1997).
- [24] D. Roman-Liu, and T. Tokarski, "Upper limb strength in relation to upper limb posture", *Int. J. Industrial Ergonomics* 35, 19–31 (2005).
- [25] A. Gedliczka, *Atlas of Human Measurements: Data for Design and Ergonomic Evaluation*, Central Institute for Labour Protection, Warsaw, 2001, (in Polish).